

# Structural and Mechanistic Comparison of Prokaryotic and Eukaryotic Phosphoinositide-specific Phospholipases C

Dirk W. Heinz<sup>1\*</sup>, Lars-Oliver Essen<sup>2</sup> and Roger L. Williams<sup>3</sup>

<sup>1</sup>*Institut für Organische Chemie und Biochemie Universität Freiburg Albertstrasse 21 D-79104, Freiburg, Germany*

<sup>2</sup>*Max-Planck-Institut für Biochemie, Abteilung Membranbiochemie, Am Klopferspitz 18a D-82152, Martinsried Germany*

<sup>3</sup>*MRC, Laboratory of Molecular Biology, Hills Road, Cambridge CB2 2QH, UK*

Phosphoinositide-specific phospholipases C (PI-PLCs) are ubiquitous enzymes that catalyse the hydrolysis of phosphoinositides to inositol phosphates and diacylglycerol (DAG). Whereas the eukaryotic PI-PLCs play a central role in most signal transduction cascades by producing two second messengers, inositol-1,4,5-trisphosphate and DAG, prokaryotic PI-PLCs are of interest because they act as virulence factors in some pathogenic bacteria. Bacterial PI-PLCs consist of a single domain of 30 to 35 kDa, while the much larger eukaryotic enzymes (85 to 150 kDa) are organized in several distinct domains. The catalytic domain of eukaryotic PI-PLCs is assembled from two highly conserved polypeptide stretches, called regions X and Y, that are separated by a divergent linker sequence. There is only marginal sequence similarity between the catalytic domain of eukaryotic and prokaryotic PI-PLCs. Recently the crystal structures of a bacterial and a eukaryotic PI-PLC have been determined, both in complexes with substrate analogues thus enabling a comparison of these enzymes in structural and mechanistic terms.

Eukaryotic and prokaryotic PI-PLCs contain a distorted ( $\beta\alpha$ )<sub>8</sub>-barrel as a structural motif with a surprisingly large structural similarity for the first half of the ( $\beta\alpha$ )<sub>8</sub>-barrel and a much weaker similarity for the second half. The higher degree of structure conservation in the first half of the barrel correlates with the presence of all catalytic residues, in particular two catalytic histidine residues, in this portion of the enzyme. The second half contributes mainly to the features of the substrate binding pocket that result in the distinct substrate preferences exhibited by the prokaryotic and eukaryotic enzymes. A striking difference between the enzymes is the utilization of a catalytic calcium ion that electrostatically stabilizes the transition state in eukaryotic enzymes, whereas this role is filled by an analogously positioned arginine in bacterial PI-PLCs.

The catalytic domains of all PI-PLCs may share not only a common fold but also a similar catalytic mechanism utilizing general base/acid catalysis. The conservation of the topology and parts of the active site suggests a divergent evolution from a common ancestral protein.

© 1998 Academic Press Limited

**Keywords:** catalytic mechanism; crystal structure; TIM-barrel; phosphoinositide-specific phospholipase; PI-PLC

\*Corresponding author

Abbreviations used: bPI-PLC, *Bacillus cereus* PI-PLC; DAG, 1,2-diacyl-*sn*-glycerol; GPI, glycosylphosphatidylinositol; GPI-PLC, glycosylphosphatidylinositol-specific phospholipase C; InsP<sub>3</sub>, *D*-myo-inositol-1-phosphate; InsP<sub>2</sub>, *D*-myo-inositol-1,4-bisphosphate; InsP<sub>3</sub>, *D*-myo-inositol-1,4,5-trisphosphate; Ins(1:2cyc)P, *D*-myo-inositol 1:2-cyclic phosphate; mPI-PLC, PI-PLC- $\delta$ 1 from rat; PI, phosphatidylinositol; PIP, phosphatidylinositol-4-monophosphate; PIP<sub>2</sub>, phosphatidylinositol-4,5-bisphosphate; PI-PLC, phosphatidylinositol-specific phospholipase C; r.m.s., root-mean-square; TIM, triose phosphate isomerase.

## Introduction

Phosphoinositide-specific phospholipases C (PI-PLC) are ubiquitous enzymes that catalyse the specific cleavage of the phosphodiester bond of phosphoinositides (PI, PIP, PIP<sub>2</sub>) to generate water-soluble inositol phosphates (InsP, InsP<sub>2</sub>, InsP<sub>3</sub>) and membrane-bound diacylglycerol (DAG; Figure 1). In higher eukaryotes, PI-PLCs are key enzymes in most receptor-mediated signal transduction pathways. They catalyse the hydrolysis of phosphatidylinositol 4,5-bisphosphate (PIP<sub>2</sub>) to generate two second messengers, inositol-1,4,5-trisphosphate (InsP<sub>3</sub>) and DAG. InsP<sub>3</sub> is released into the cytoplasm and results in influx of Ca<sup>2+</sup> from internal stores, whereas DAG remains membrane resident and stimulates protein kinase C isozymes (Nishizuka, 1992; Berridge, 1993). Mammalian PI-PLCs have been classified into three families based on their primary structure and mode of activation: the β-family (150 kDa) is activated by association with heterotrimeric G-protein subunits, the γ-family (145 kDa) is activated by association with tyrosine kinases, and the simpler δ-family (85 kDa) for which regulation *in vivo* remains largely unknown. The mammalian PI-PLCs are strictly dependent on Ca<sup>2+</sup> and show a clear substrate preference in the order PIP<sub>2</sub> > PIP ≫ PI (reviewed by Bruzik & Tsai, 1994).

The crystal structure of the mammalian PLC-δ1 (Essen *et al.*, 1996) shows that the enzyme has a multidomain organisation consisting of a catalytic domain and a set of accessory domains including a PH domain (Ferguson *et al.*, 1995), an EF-hand domain, and a C2 domain. These accessory domains facilitate interactions with membranes and other components of the cell signalling systems, and are shared with many proteins involved in signal transduction. The catalytic domain has a fold that consists of a distorted eight-stranded (β<sub>α</sub>)<sub>8</sub>-barrel (TIM-barrel). The TIM-barrel topology is common to many enzymes, but the arrangement of the active site is unique to PI-PLC. The catalytic domain is the most conserved portion of eukaryotic PI-PLCs (Rhee *et al.*, 1989; Williams & Katan, 1996), with the N-terminal half of the barrel

(originally denoted the X-region) more conserved than the C-terminal half (originally denoted the Y-region). The two halves of the TIM-barrel are linked by an insertion (X/Y linker) that is highly variable in sequence and length, ranging from 40 to 480 residues. In PLC-γ isozymes the X/Y linker region contains an SH2/SH2/SH3/split PH domain array that is responsible for stimulation of the enzyme by tyrosine kinases.

PI-PLCs with much smaller molecular masses, ranging from 30 kDa to 35 kDa are secreted in large quantities by bacteria such as *Bacillus cereus*, *B. thuringiensis*, *Staphylococcus aureus*, and *Listeria monocytogenes* (Ikezawa, 1991). They play a role as virulence factors in pathogenic bacteria (Mengaud *et al.*, 1991; Leimeister-Wächter *et al.*, 1991; Daugherty & Low, 1993), but in most cases their precise physiological function remains elusive. In contrast to their mammalian counterparts, they do not require Ca<sup>2+</sup> for activity. They also do not hydrolyse PIP or PIP<sub>2</sub>. The cleavage of PI, however, occurs at rates about ten times faster than for mammalian PI-PLCs (Bruzik & Tsai, 1994), about the same as the rate at which eukaryotic PI-PLCs hydrolyse PIP or PIP<sub>2</sub> (Ellis & Katan, 1995). The crystal structure of the PI-PLC from *B. cereus* (Heinz *et al.*, 1995) shows that this enzyme consists of a single domain with a TIM-barrel type architecture, which is very similar to the catalytic domain of the mammalian enzyme. There is only a limited sequence similarity between the bacterial and mammalian PI-PLCs, with 26% similarity in the N-terminal-half of the catalytic domain and no detectable similarity in the C-terminal half (Kuppe *et al.*, 1989).

A distinctly different type of eukaryotic phospholipase C is the glycosylphosphatidylinositol-specific PLC (GPI-PLC) expressed by the human pathogenic parasite *Trypanosoma brucei*. Unlike other eukaryotic PI-PLCs, this 39 kDa enzyme behaves like an integral membrane protein (Hereld *et al.*, 1988). In many respects, however, this enzyme is more similar to prokaryotic PI-PLCs than other eukaryotic PI-PLCs. It is metal-independent and hydrolyses the GPI-anchor of variant surface glycoprotein or GPI biosynthetic intermediates

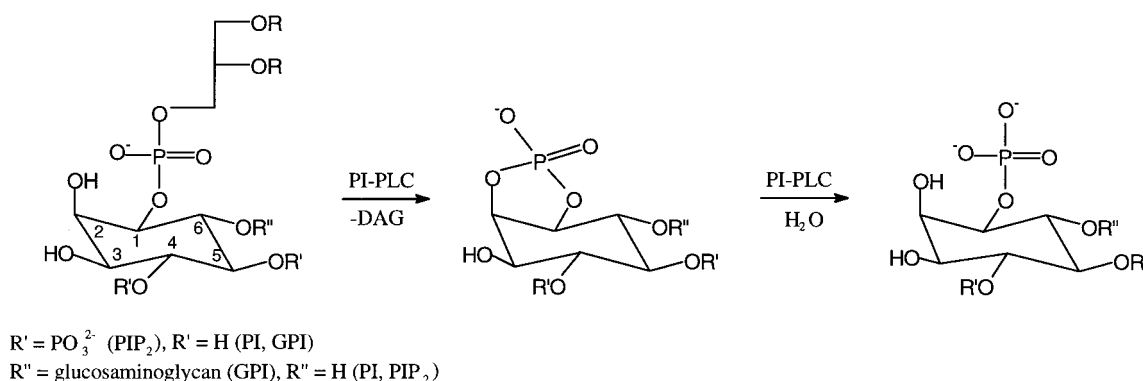


Figure 1. The two-step reaction catalysed by PI-PLC.

(Carrington *et al.*, 1991; Morris *et al.*, 1995). Besides GPI, the enzyme also cleaves PI but not the phosphorylated phosphoinositides PIP and PIP<sub>2</sub> (Bütikofer *et al.*, 1996). It also has a greater sequence similarity to the N-terminal half of the *B. cereus* PI-PLC (34%) than to the same region of the mammalian PI-PLCs (<10%) (Carrington *et al.*, 1991; Mengaud *et al.*, 1991).

Having the structures of both a eukaryotic and a prokaryotic PI-PLC as well as an extensive set of prokaryotic and eukaryotic PI-PLC sequences offers the opportunity to better understand the relationship between structure and enzymatic activity for this class of enzymes. Based on the comparison of these structures we propose a structural model for the catalytic domains of all PI-PLCs. In addition the strong structural conservation of one half of the catalytic domain that harbours almost all of the catalytically important residues and the similarities in the mechanism of catalytic action suggest that pro- and eukaryotic PI-PLCs are descendants from a common ancestor.

## Results and Discussion

### The PI-PLC fold

The crystal structures of PI-PLC from *Bacillus cereus* (bPI-PLC; PDB entry code 1PTD) and PI-

PLC- $\delta$ 1 from rat (mPI-PLC; entry code 2ISD) that were determined in uncomplexed forms and in complex with various substrate analogues (entry codes: 1PTG, 1GYM, 1DJX, 1DJW, 1DJY and 1DJZ) were reported elsewhere (Heinz *et al.*, 1995, 1996; Essen *et al.*, 1996, 1997). Whereas bPI-PLC folds as a single domain of 298 residues, mPI-PLC consists of four domains (PH domain, EF-hand domain, catalytic domain and C2 domain) comprising 756 amino acid residues.

Based on their overall topologies both bPI-PLC and the catalytic domain of mPI-PLC (308 residues) can be described as "cousins" belonging to the large structural superfamily of ( $\beta\alpha$ )<sub>8</sub>-barrels (TIM-barrels) which includes roughly 10% of all known enzyme structures (Reardon & Farber, 1995). Both structures diverge from the regular TIM-barrel fold that consists of eight ( $\beta\alpha$ )-units, where the parallel  $\beta$ -strands (I to VIII) form a strictly closed circular structure.

In bPI-PLC, two  $\alpha$ -helices expected to be located between strands IV and V and strands V and VI are lacking (Figure 2, Table 1). In addition,  $\beta$ -strands V and VI are too far away from each other to allow the formation of main-chain hydrogen bonds. Consequently this leads to an opening of the barrel in this area. A portion of the missing hydrogen-bonding potential is compensated by an

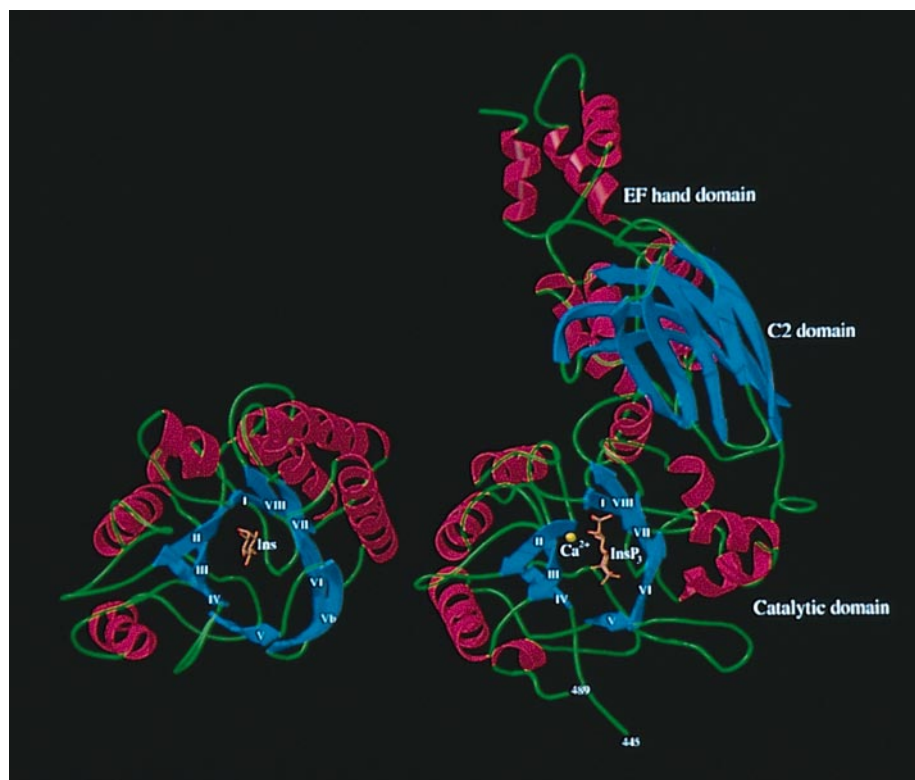


**Figure 2.** Ribbon plots of the crystal structures of bPI-PLC (left picture) and mPI-PLC (right picture). The view is into the active site pocket with Ins (orange bonds) bound to bPI-PLC and InsP<sub>3</sub> (orange bonds) bound to the catalytic domain of mPI-PLC.  $\alpha$ -Helices are shown in red,  $\beta$ -strands in blue and loops in green;  $\beta$ -strands in the catalytic domains are labelled with Roman numbers. The Ca<sup>2+</sup> located in the active site of mPI-PLC is indicated by a yellow sphere. This Figure, as well as Figures 3, 4, 6 and 9 were prepared using the programs MOLSCRIPT (Kraulis, 1991) and RASTER3D (Merrit & Murphy, 1994).

**Table 1.** Secondary structure positions in bPI-PLC and mPI-PLC and sequence alignment based on their structural superposition

Secondary structure element	bPI-PLC <sup>a</sup>	mPI-PLC <sup>a</sup>	r.m.s. difference of common C <sup>α</sup> position (Å) (number of common C <sup>α</sup> -positions)
<b>α-Helix</b>			
1''	3–8 (A)	–	–
1'	42–48 (B)	–	–
1	54–62 (C)	326–336 (Tα1)	1.64 (9)
2	90–102 (D)	365–377 (Tα2)	2.02 (12)
3	129–139 (E)	394–412 (Tα3)	2.64 (9)
4	–	490–495 (Tα4)	–
5	–	–	–
6	205–222 (F)	525–534 (Tα5)	2.24 (5)
6'	–	536–545 (Tα5')	–
7	243–263 (G)	564–570 (Tα6)	>4
8	284–294 (H)	584–595 (Tα7)	>4
<b>β-Strand</b>			
I	26–33	306–312 (Tβ1)	0.92 (7)
II	63–71	337–345 (Tβ2)	1.00 (9)
III	107–116	382–392 (Tβ3)	1.19 (10)
IV	156–163	433–440 (Tβ4)	1.15 (8)
V	173–178	498–503 (Tβ5)	3.36 (6)
Vb	182–188	–	–
VI	193–200	518–524 (Tβ6)	1.10 (5)
VII	226–235	546–552 (Tβ7)	0.98 (7)
VIII	269–273	573–578 (Tβ8)	1.06 (6)

<sup>a</sup> Label in parentheses is the label used in the original publication of the structure description.

additional β-strand (Vb) that lines up with strand VI in an antiparallel fashion. The TIM-barrel is not circular but rather elliptical with distances between C<sup>α</sup>-atoms in opposite strands ranging from 12 to 18 Å. The length distribution of the β-strands forming the barrel is rather uneven ranging from five residues for strand VIII up to ten residues for strand VII with an average of 8.7 residues per strand.

In mPI-PLC, the TIM-barrel comprising the catalytic domain (residues 299 to 606) is closed but also distorted with an α-helix missing between strands V and VI. The barrel is elliptical but more compact than bPI-PLC with distances between C<sup>α</sup>-atoms in opposite strands ranging from 9.5 to 14 Å (Figure 2, Table 1). The length of the β-strands tends to be shorter with an average of 7.6 residues per strand. In mPI-PLC, a disordered stretch of 45 mostly polar residues (X/Y-linker) connects two halves of the TIM-barrel. In both PI-PLCs, neighbouring β-strands are tilted relative to each other by about –35° and have a shear number of eight encircling the barrel (McLachlan, 1979). Using the DALI algorithm for 3D structure comparisons (Holm & Sander, 1993), the highest scoring similar structures were all TIM-barrel containing proteins. Searching separately with the X and Y-regions resulted in a significantly higher number of structures aligning to the X-region.

The PI-PLCs show no structural similarity to other phospholipases, e.g. phospholipases A<sub>2</sub> (e.g. White *et al.*, 1990), a phosphatidylcholine-hydrolysing phospholipase C (Hough *et al.*, 1989), or lipases (for a review see Cambillau & van Tilbeurgh, 1993). PI-PLCs are the first known TIM-barrel containing enzymes that interact with lipid mem-

branes. The distortions from an ideal TIM-barrel fold in both PI-PLCs might be dictated by the steric requirements to dock a TIM-barrel domain on a phospholipid membrane and to allow the entry of phospholipid head groups into the active site or the release of product following catalysis. Irregularities in a TIM-barrel topology are also found for a cellobiohydrolase (Rouvinen *et al.*, 1990) and an endocellulase (Spezio *et al.*, 1993). These enzymes also interact with large substrates and deviate from the canonical TIM-barrel fold by missing secondary structure elements as well.

### Superposition of bPI-PLC and mPI-PLC and a structure-based sequence alignment

When the structures of bPI-PLC and the catalytic domain of mPI-PLC were superimposed (Figure 3), an excellent fit was found for the N-terminal halves (residues 1 to 163 of bPI-PLC and residues 299 to 440 of mPI-PLC) with an r.m.s. deviation of 1.85 Å for 104 equivalent C<sup>α</sup>-positions (Table 1, Figure 3). For this region, the topology of the secondary structure elements is basically identical (Figure 4) with the exception of two additional short α-helices present only in bPI-PLC (residues 3 to 8 and 42 to 48). Amino acid insertions and deletions are mainly restricted to loops. In particular, β-strands I to IV aligned very well with an r.m.s. deviation of 1.1 Å for 32 equivalent C<sup>α</sup>-positions. The α-helices following β-strands I to III also aligned reasonably well with an r.m.s. deviation of 1.9 Å for 26 common C<sup>α</sup>-positions. The extended loop following β-strand II (residues 73 to 90 in bPI-PLC, residues 346 to 364 in mPI-PLC) shows a

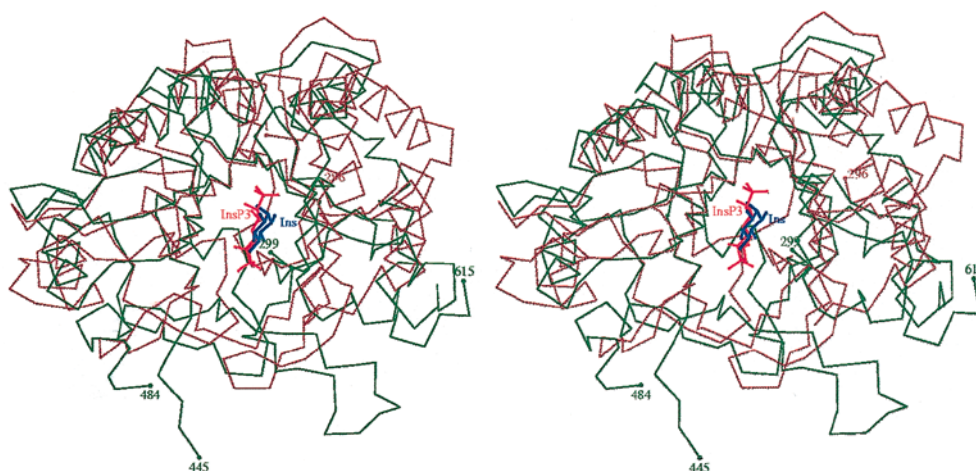


**Figure 3.** Stereo pair showing the superposition of the C $\alpha$ -traces of bPI-PLC (residues 1 to 296; coloured brown) and the catalytic domain of mPI-PLC (residues 299 to 615; coloured green). The view is into the active site pocket with an InsP<sub>3</sub> molecule (coloured red) and Ins (coloured blue) bound to the active sites of mPI-PLC and bPI-PLC, respectively. Residues located between position 445 and 484 in mPI-PLC are disordered and not shown.

strikingly similar conformation despite its length. This loop contributes a residue that is essential for catalysis (His82 in bPI-PLC, His356 in mPI-PLC).

Much larger positional deviations were found for the C-terminal halves of bPI-PLC (residues 164

to 296) and mPI-PLC (residues 490 to 610) with an r.m.s. deviation of 2.9 Å for only 39 equivalent C $\alpha$ -positions (Figure 4, Table 1). The best agreement was found for  $\beta$ -strands V to VIII that show an r.m.s. deviation of 2.5 Å for 27 equivalent C $\alpha$ -pos-

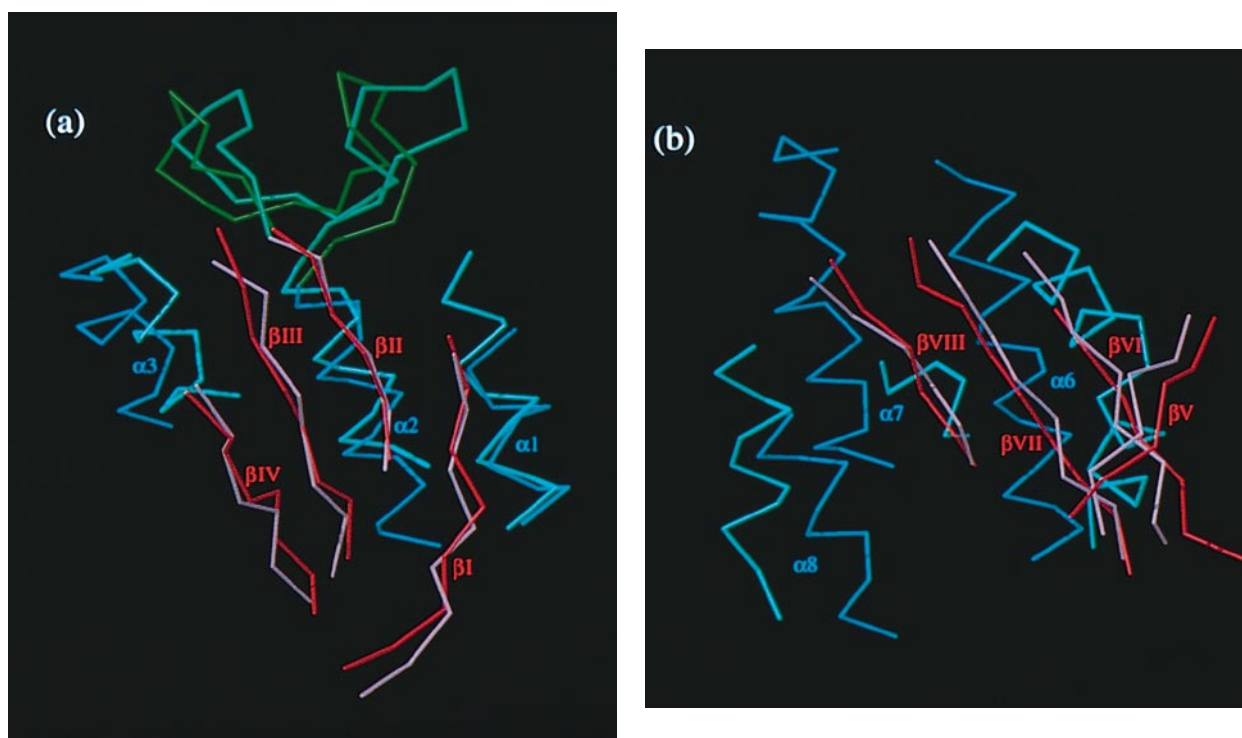
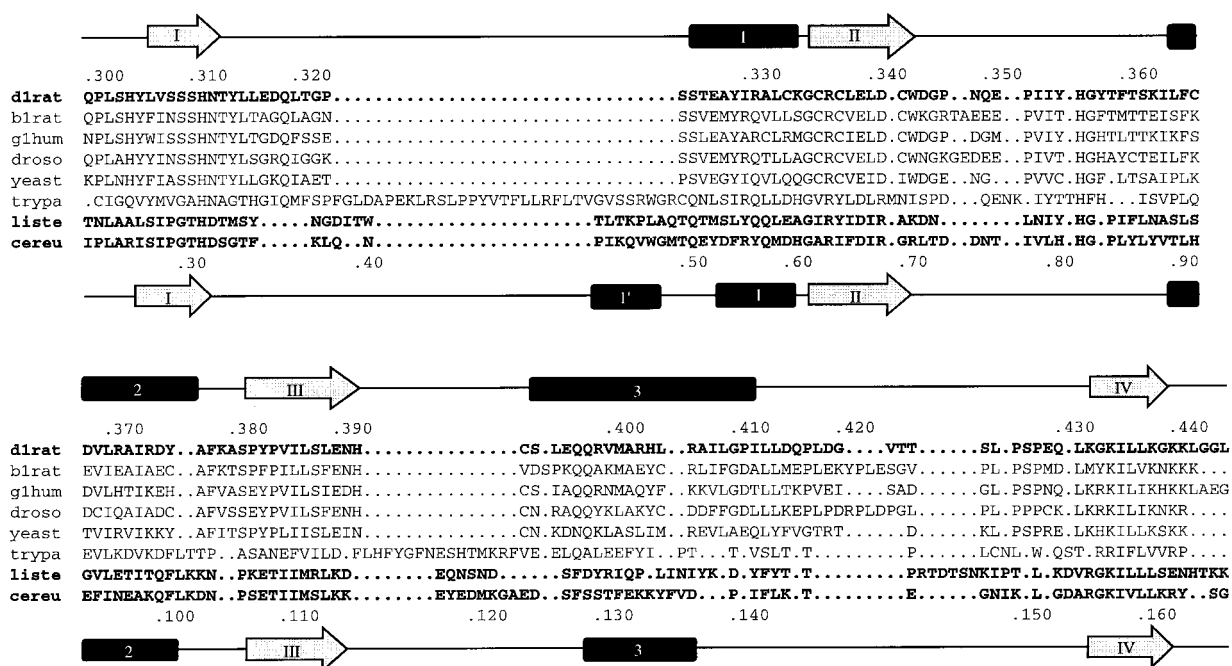


**Figure 4.** Superposition of secondary structure elements of mPI-PLC and bPI-PLC. Shown are C $\alpha$ -traces where  $\beta$ -strands are coloured red,  $\alpha$ -helices blue and loops green. The colour shading is darker in the case of bPI-PLC. (a) Region X: Shown are the C $\alpha$ -positions of residues 25 to 32 ( $\beta$ I), 65 to 70 ( $\beta$ II), 109 to 116 ( $\beta$ III), 155 to 162 ( $\beta$ IV), 54 to 62 ( $\alpha$ 1), 91 to 104 ( $\alpha$ 2), 129 to 139 ( $\alpha$ 3) and 70 to 91 (loop connecting  $\beta$ II and  $\alpha$ 2) belonging to bPI-PLC and residues 304 to 311 ( $\beta$ I), 339 to 344 ( $\beta$ II), 384 to 391 ( $\beta$ III), 433 to 439 ( $\beta$ IV), 325 to -336 ( $\alpha$ 1), 366 to 376 ( $\alpha$ 2), 398 to 408 ( $\alpha$ 3) and 344 to 366 (loop connecting  $\beta$ II and  $\alpha$ 2) belonging to mPI-PLC. (b) Region Y: Shown are the C $\alpha$ -positions of residues 172 to 177 ( $\beta$ V), 191 to 197 ( $\beta$ VI), 226 to 234 ( $\beta$ VII), 269 to 274 ( $\beta$ VIII), 204 to 222 ( $\alpha$ 6), 245 to 263 ( $\alpha$ 7), 285 to 294 ( $\alpha$ 8) belonging to bPI-PLC and residues 498 to 503 ( $\beta$ V), 517 to 524 ( $\beta$ VI), 545 to 552 ( $\beta$ VII), 573 to 578 ( $\beta$ VIII), 525 to 544 ( $\alpha$ 6), 564 to 569 ( $\alpha$ 7), 586 to 596 ( $\alpha$ 8) belonging to mPI-PLC.

## Region X:



## Region Y:

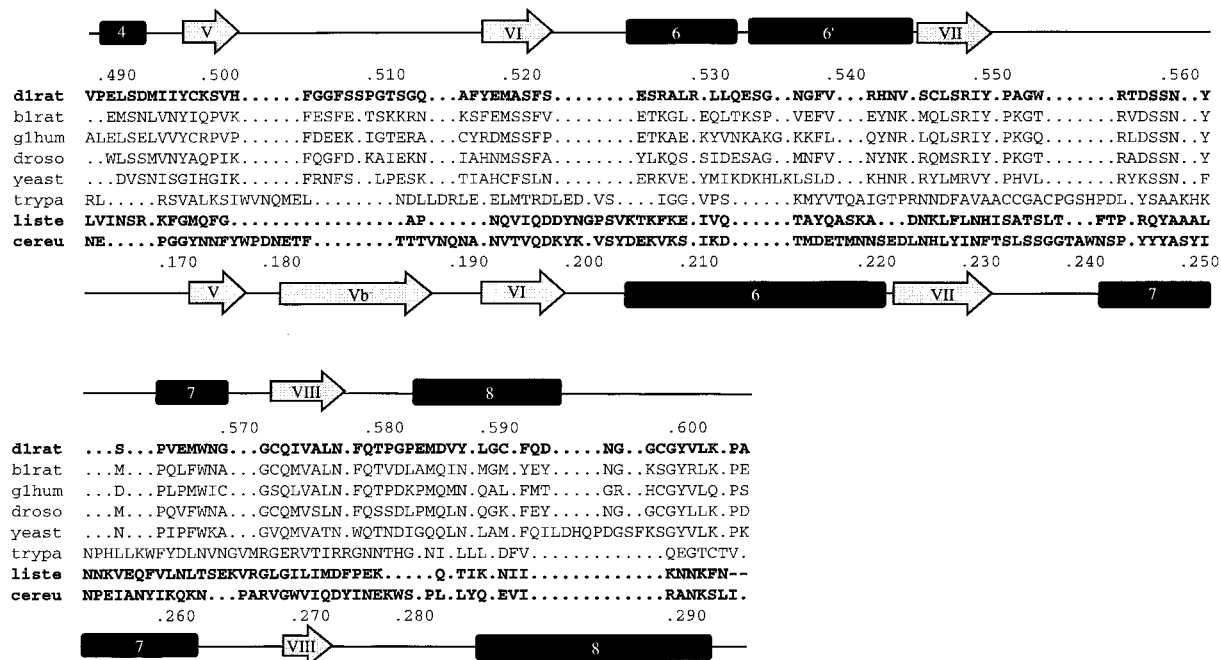


**Figure 5.** Multiple sequence alignment of eukaryotic and prokaryotic PI-PLCs for regions X (upper panel) and Y (lower panel). Listed from the top to the bottom are the following PI-PLCs: PI-PLC- $\delta 1$  from rat (d1rat), PI-PLC- $\beta 1$  from rat (blrat), human PI-PLC- $\gamma 1$  (glhum), PI-PLC from *Drosophila* (droso), PI-PLC from yeast (yeast), PI-PLC from *T. brucei* (trypa), PI-PLC from *L. monocytogenes* (liste) and PI-PLC from *B. cereus* (cereu). The alignment of the rat PI-PLC- $\delta 1$  with respect to *B. cereus* PI-PLC is based on the bPI-PLC and mPI-PLC structures in regions where the structures superimpose well. The alignment of bPI-PLC and PI-PLC from *L. monocytogenes* (liste) is structure-based as well (Moser *et al.*, 1997). The alignment of the other sequences with respect to these was based on an automatic sequence alignment that was manually adjusted. The secondary structure elements of each structure are shown above and below the sequences, respectively;  $\alpha$ -helices are symbolized as black rectangles,  $\beta$ -strands as grey arrows. Amino acids 443 to 487 in mPI-PLC are part of the X/Y linker and are not shown. Every tenth amino acid is numbered for mPI-PLC (top) and bPI-PLC (bottom).

itions. In contrast, the  $\alpha$ -helices show substantial deviations in their length and relative orientation to the  $\beta$ -barrel.

Figure 5 shows a multiple sequence alignment of PI-PLCs based on the structure-based sequence alignment of mPI-PLC and bPI-PLC. Despite a very similar overall topology the sequence identity between mPI-PLC and bPI-PLC is only around 5% with a significantly higher conservation for residues belonging to the first half of the barrel (11%). In this half sequence identity was found for 16 residue-pairs. Based on their location and role in the structure these residues can be subdivided into three groups. The first group comprises residues contributing to the active site, i.e. the catalytic histidine (H311/H32 and H356/H82) as well as a glycine residue (G357/G83) that probably directs *via* its increased conformational freedom the second catalytic histidine in a position optimal for protonation of the leaving group DAG during catalysis. In addition there is a conserved serine (S388/S113) that participates in the formation of the active site pocket without directly interacting with the substrate. The second group includes seven apolar residues forming the hydrophobic core of the protein (Table 2) as well as a completely buried arginine residue (R338/R64) that "closes" the hydrophobic core at the N-terminal side of the  $\beta$ -barrel *via* multiple hydrogen bonds with neighbouring main-chain carbonyl groups. Mutation of this residue (R338L) in mPI-PLC completely inactivates the enzyme, probably by destabilizing the barrel (Table 4). Finally conservation is also found for a proline (P301/P22) and two glycine residues (G336/G62; G433/G156) that are located in tight turns preceding  $\beta$ -strands. No obvious role could

be attributed to a conserved lysine (K434/K157) located at the surface of the protein far away from the active site.

The number of conservative replacements in the N-terminal half is significantly higher (32%) than the sequence identity. This applies particularly to the hydrophobic mini-core wedged between the  $\beta$ -strands and  $\alpha$ -helices (Table 2). When considering secondary structure elements alone the conservation of amino acids is clearly concentrated on  $\beta$ -strands I to IV of the central  $\beta$ -barrel (approx. 60%) whereas the amphipathic helices and loops show a significantly higher variability (Figure 5).

Unlike the N-terminal half, no apparent conservation is found for the C-terminal half of the TIM-barrel, not even for residues belonging to the spatially conserved  $\beta$ -strands V to VIII. In mPI-PLC, most contacts of the catalytic domain with the neighbouring C2 domain are made by the surface helices of the C-terminal half of the barrel with an area of approximately 1800 Å<sup>2</sup> buried between the two domains. This means that roughly 9% of the total surface area of the catalytic domain is buried in this rigid (Grobler *et al.*, 1996) interface. The absence of any additional domains in bPI-PLCs apparently results in a larger structure and sequence divergence of the surface helices in the C-terminal half of the barrel.

### Extension of the structure based sequence alignment to other PI-PLCs

One goal of this study was to use the structure based alignment of the catalytic domains of bacterial and eukaryotic PI-PLCs to extend it to the remaining PI-PLCs for which no crystal structures

**Table 2.** Conservation of the hydrophobic mini-cores belonging to the N-terminal half of the TIM-barrels of bPI-PLC and mPI-PLC

Residue in bPI-PLC	Residue in mPI-PLC	Positional difference of C <sup>α</sup> -positions (Å)	Location in secondary structure
<b>L23</b>	<b>L302</b>	2.31	Loop preceding $\beta$ I
M59	L333	1.21	$\alpha$ 1
F66	L340	0.80	$\beta$ II
I68	L342	1.14	$\beta$ II
I78	P352	1.53	Loop between $\beta$ II and $\alpha$ 2
V79	I353	0.70	Loop between $\beta$ II and $\alpha$ 2
L80	I354	0.43	Loop between $\beta$ II and $\alpha$ 2
V89	I364	1.84	Loop between $\beta$ II and $\alpha$ 2
L91	F366	1.53	$\alpha$ 2
F94	V369	1.99	$\alpha$ 2
I95	L370	1.55	$\alpha$ 2
A98	I373	1.70	$\alpha$ 2
I110	V385	0.99	$\beta$ III
<b>I111</b>	<b>I386</b>	0.60	$\beta$ III
M112	L387	0.34	$\beta$ III
<b>L114</b>	<b>L389</b>	0.35	$\beta$ III
<b>I141</b>	<b>I412</b>	2.45	Loop between $\alpha$ 3 and $\beta$ IV
F142	L413	1.57	Loop between $\alpha$ 3 and $\beta$ IV
<b>L143</b>	<b>L414</b>	0.55	Loop between $\alpha$ 3 and $\beta$ IV
A154	L431	1.90	Loop between $\alpha$ 3 and $\beta$ IV
<b>I158</b>	<b>I435</b>	0.97	$\beta$ IV
V159	L436	0.98	$\beta$ IV
<b>L160</b>	<b>L437</b>	0.60	$\beta$ IV

Conserved residues are shown bold-face.

**Table 3.** Hydrogen bonding interactions between bPI-PLC and mPI-PLC and the inositols Ins and InsP<sub>3</sub>, respectively

Atoms in inositols	Residue and atom (distance in Å)	
	In bPI-PLC	In mPI-PLC
O1	–	–
O7 of 1-phosphate group	–	His356 N <sup>ε2</sup> (2.6)
O9 of 1-phosphate group	–	His311 N <sup>ε2</sup> (2.8)
	–	Asn312 O <sup>δ1</sup> (2.8)
O2	His32 N <sup>ε2</sup> (3.1)	Glu390 O <sup>ε1</sup> (3.2)
	Arg69 NH <sup>ε2</sup> (2.9)	Ca <sup>2+</sup> (2.4)
O3	Asp198 O <sup>δ1</sup> (2.8)	Glu341 O <sup>ε1</sup> (2.5)
	–	Glu341 O <sup>ε2</sup> (2.9)
	–	Arg549N <sup>ε1</sup> (3.1)
O4	Arg163 N <sup>ε1</sup> (3.2)	–
	Arg163 N <sup>ε2</sup> (3.0)	–
	Asp198 O <sup>δ2</sup> (2.6)	–
O12 of 4-phosphate group	–	Lys438 N <sup>ε</sup> (3.0)
	–	Ser522 O <sup>γ</sup> (2.6)
	–	Arg549 N <sup>ε1</sup> (3.1)
O5	Arg163 N <sup>ε2</sup> (2.8)	–
O14 of 5-phosphate group	–	Lys440 N <sup>ε</sup> (4.1)
O6	–	–

yet exist. The multiple sequence alignment shown in Figure 5 includes one representative of mammalian  $\beta$ ,  $\gamma$ , and  $\delta$ -isozymes, the PI-PLCs from insect, yeast, *T. brucei* and two bacterial species.

The alignments of eukaryotic and prokaryotic PI-PLCs were performed separately and later com-

bined and manually optimized according to the structure based sequence alignment of bPI-PLC and mPI-PLC. The sequence identity among eukaryotic PI-PLCs (except for *T. brucei* PI-PLC) was about 60% for the X-region of the barrel and about 40% for the Y-region. Therefore the much

**Table 4.** Catalytic activity of bacterial and mammalian PI-PLC mutants

Mutant	mPI-PLC equivalent	Catalytic activity (% of wild-type activity) towards substrates PI or PIP <sub>2</sub>	Remarks	Reference
H311A (rat- $\delta$ 1)	H311	<0.1 (PI), <0.1 (PIP <sub>2</sub> )	Catalytic histidine	Ellis & Katan (1995)
H335F (rat- $\delta$ 1)	H311	<10% (PIP <sub>2</sub> )	Catalytic histidine	Smith <i>et al.</i> (1994)
R338L (hum- $\delta$ 1)	R338	<0.1 (PI), <0.1 (PIP <sub>2</sub> )	TIM barrel closure	Cheng <i>et al.</i> (1995)
E341G (hum- $\delta$ 1)	E341	<0.1 (PI), <0.1 (PIP <sub>2</sub> )	Ca <sup>2+</sup> ligand	Cheng <i>et al.</i> (1995)
H380F (rat- $\gamma$ 1)	H356	<10% (PIP <sub>2</sub> )	Catalytic acid	Smith <i>et al.</i> (1994)
H356A (rat- $\delta$ 1)	H356	<0.1 (PI), <0.1 (PIP <sub>2</sub> )	Catalytic acid	Katan, M. (unpublished)
H356L (hum- $\delta$ 1)	H356	<0.1 (PI), <0.1 (PIP <sub>2</sub> )	Catalytic acid	Cheng <i>et al.</i> (1995)
K440Q (hum- $\delta$ 1)	K440	106 (PI), 105 (PIP <sub>2</sub> )	Salt-bridge to 5-phosphoryl of PIP <sub>2</sub>	Cheng <i>et al.</i> (1995)
K461R (hum- $\beta$ 2)	K438	<0.1 (PIP <sub>2</sub> )	Salt-bridge to 4-phosphoryl of PIP <sub>2</sub>	Simões <i>et al.</i> (1995)
K463R (hum- $\beta$ 2)	K440	20 (PIP <sub>2</sub> )	Salt-bridge to 5-phosphoryl of PIP <sub>2</sub>	Simões <i>et al.</i> (1995)
R549G (hum- $\delta$ 1)	R549	19 (PI), <0.1 (PIP <sub>2</sub> )	Salt-bridge to 4-phosphoryl of PIP <sub>2</sub>	Cheng <i>et al.</i> (1995)
H32L (bPI-PLC)	H311	0.0005 (PI)	Catalytic base	Heinz <i>et al.</i> (1995)
R69K (bPI-PLC)	D343	0.002 (PI)	Negative charge stabilization during catalysis	Gässler <i>et al.</i> (1997)
H82L (bPI-PLC)	H356	0.007 (PI)	Catalytic acid	Heinz <i>et al.</i> (1995)
D274S (bPI-PLC)	N578	<0.9 (PI)	Member of "catalytic triad"	Gässler <i>et al.</i> (1997)

higher sequence similarity among eukaryotic PI-PLCs suggests virtually identical three-dimensional structures for the catalytic domains of all eukaryotic PI-PLCs. The alignment of bPI-PLC and PI-PLC from *L. monocytogenes*, the crystal structure of which was determined very recently (Moser *et al.*, 1997), is structure-based resulting in a sequence identity of 24%. Despite this relatively weak conservation both enzymes share a very similar three-dimensional structure (Moser *et al.*, 1997). The alignment of *T. brucei* GPI-PLC with bPI-PLC (Figure 5) shows a sequence identity of 20% for the N-terminal half of the protein and 13% for the C-terminal half. When compared with the mammalian PI-PLCs, *T. brucei* GPI-PLC shows a strongly reduced similarity for the N-terminal half and almost no similarity in the C-terminal half. Based on this sequence analysis and additional secondary structure predictions, one can conclude that the structure of the N-terminal half of *T. brucei* GPI-PLC is more closely related to the bacterial PI-PLCs, whereas the C-terminal half might have no structural equivalent among eukaryotic and prokaryotic PI-PLCs. Despite the weak sequence homology between eukaryotic and prokaryotic PI-PLCs, based on the present structural comparison it is very likely that the catalytic domains of all PI-PLCs share a common fold.

### Substrate specificity

The structures of PI-PLCs in complexes with substrate-analogues have resulted in a simple framework for understanding a host of kinetic observations of the enzymes. The structures show that almost all of the mutations reported to inactivate the enzyme are mutations of residues that make specific contacts with the substrate or cofactor (Table 4). The observed interactions in the active site also clarify the origin of the substrate prefer-

ences that have been noted for bPI-PLC and mPI-PLC.

Like other TIM-barrel enzymes, the active site of PI-PLCs is located at the C-terminal end of the  $\beta$ -barrel forming a relatively wide, open cleft. The active sites have been delineated in the structures of bPI-PLC (Heinz *et al.*, 1995) and mPI-PLC (Essen *et al.*, 1996) *via* the binding of the inositol head group of their natural substrates, PI and  $\text{PIP}_2$ , respectively, as well as modified inositols (Heinz *et al.*, 1996; Essen *et al.*, 1997).

In both PI-PLCs, the inositols bind in an edge-on mode to the active site (Figure 6). Upon complexation, 83% of the Ins surface is buried from solvent in bPI-PLC whereas 53% of  $\text{InsP}_3$  is buried in mPI-PLC. Both inositols are stereospecifically recognized *via* interactions between their hydroxyls (and their phosphate groups in the case of  $\text{InsP}_3$ ) and side-chains of polar and charged amino acids (Table 3). In addition, there is a coplanar stacking interaction between the apolar side of the inositol ring and the aromatic side-chain of a tyrosine residue (Tyr551 in mPI-PLC and Tyr200 in bPI-PLC). This mode of binding resembles interactions observed between carbohydrate binding proteins and their substrates (Quiocho, 1989). There are no close interactions between main-chain atoms and the inositol in either enzyme. All residues in bPI-PLC interacting with Ins are also conserved in PI-PLC from *S. aureus* (Daugherty & Low, 1993) and *L. monocytogenes* (with the exception of Arg163: Leimeister-Wächter *et al.*, 1991; Moser *et al.*, 1997). Similarly, the amino acids in the active site of mPI-PLC interacting with  $\text{InsP}_3$  are conserved in all known eukaryotic PI-PLCs. In marked contrast to bPI-PLC, mPI-PLC binds a  $\text{Ca}^{2+}$ -cofactor that is liganded not only by a number of mostly negatively charged amino acids but also by the 2-OH-group of  $\text{InsP}_3$ . This cofactor is an essential element of catalysis (see below).

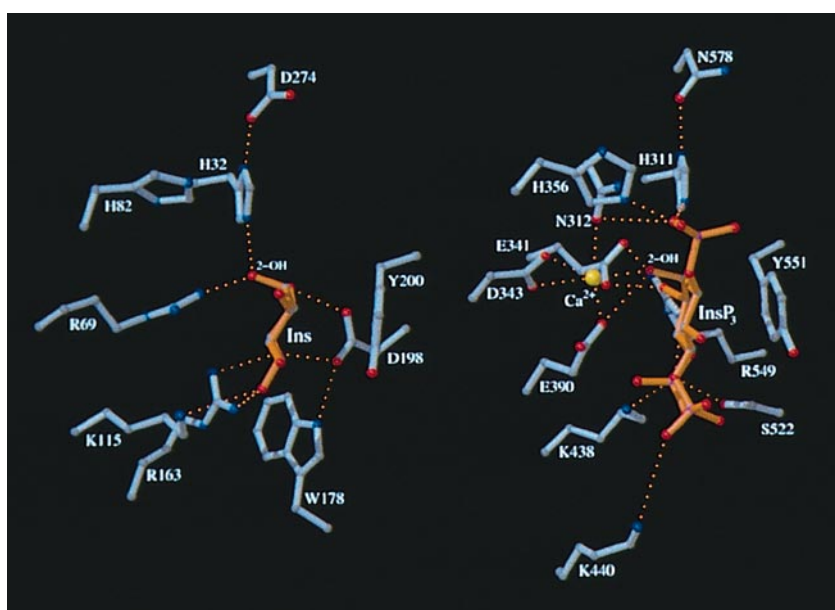


**Figure 6.** A side-by-side comparison of the active sites of bPI-PLC and mPI-PLC. Shown on the left are side-chains of residues in bPI-PLC that interact with the bound Ins (orange bonds). The right panel shows side-chains of residues in mPI-PLC that interact with  $\text{InsP}_3$  (orange bonds) and the  $\text{Ca}^{2+}$  cofactor (yellow sphere). Broken lines indicate possible hydrogen bonds.

Most amino acids that directly interact with the inositol are located in analogous  $\beta$ -strands and loops in both PI-PLCs with the exception of Asp198 and Tyr200 that are located in  $\beta$ -strand VI in bPI-PLC whereas the similarly positioned amino acids Arg549 and Tyr551 come from  $\beta$ -strand VII in mPI-PLC. Despite this difference, the side-chains of both tyrosine residues are analogously positioned in the active site to form one side of the inositol binding pocket. The fact that these residues stem from the C-terminal half (or Y-region) of the TIM-barrel that shows no obvious amino acid conservation is a further indication that the Y-regions of both enzymes diverged much further during evolution than the X-regions. This also shows that the structural requirements for substrate binding are less stringent than for catalysis.

The highly specific recognition of the inositols by both PI-PLCs observed in structural studies is supported by kinetic data using modified inositols (reviewed by Bruzik & Tsai, 1994; Potter & Lampe, 1995). The 1D-configuration of *myo*-PI substrates is absolutely required for both mammalian and bacterial PI-PLCs (Lewis *et al.*, 1993; Bruzik *et al.*, 1994; Martin & Wagman, 1996). The structures of both enzymes show that the 2- and 3-hydroxyls make several hydrogen bonds with the enzyme. The importance of the 2-hydroxyl group is consistent with the observation that the 2-methoxy inositol-substituted PI is not a substrate for bPI-PLC (Lewis *et al.*, 1993; Martin & Wagman, 1996) and that 2-deoxy inositol PI is not a substrate for human PI-PLC (Bruzik & Tsai, 1994). Inversion of the 3-hydroxyl in natural PI leads to a  $10^3$ -fold reduction of bPI-PLC-activity (Bruzik & Tsai, 1994). Furthermore, phosphoinositides phosphorylated at the 3-hydroxyl are not substrates for the mammalian PI-PLC (Serunian *et al.*, 1989; Williams & Katan, 1996).

Both PI-PLCs lack stereospecificity towards the DAG-moiety, which suggests that the hydrophobic part of PI-substrates is not specifically recognized by the enzymes (Bruzik *et al.*, 1992). Lysophosphatidylinositol and other single chain esters of inositol-1-phosphate are hydrolysed by bacterial PI-PLCs, though at reduced rates (Bruzik & Tsai, 1994). These data are supported by the present crystal structures that do not show a preformed hydrophobic channel for the specific interaction with acyl chains such as seen in phospholipases A<sub>2</sub> (Scott *et al.*, 1990), but rather a broad and shallow cleft extending from the active site pocket that could easily accommodate different DAG stereoisomers.

Phosphatidylinositol is the common ground shared by the prokaryotic and eukaryotic PI-PLCs. However, both enzymes have unique substrate specificities not shared: only the eukaryotic PI-PLCs can hydrolyse PIP and PIP<sub>2</sub>, and only the bacterial PI-PLCs can hydrolyse phospholipids glycosylated at the 6-hydroxyl position of the inositol ring. The 4- and 5-phosphoryl groups of PIP<sub>2</sub> are specifically recognized by mPI-PLC *via* positively

charged amino acids (Lys438, Lys440 and Arg549). It was shown by site-directed mutagenesis that Lys438 (Simões *et al.*, 1995) and Arg549 (Cheng *et al.*, 1995; Wang *et al.*, 1996: Table 4) are critically required for hydrolysis of PIP<sub>2</sub>, but not of PI. No analogously positioned basic residues are present in bPI-PLC. The 4- and 5-phosphoryl groups also make interactions with ordered water molecules belonging to a large solvent cluster in the wide active site of mPI-PLC. The high number of specific interactions with the 4-phosphoryl group explains the observed substrate preference of mPI-PLC for phosphorylated PIs (Ryu *et al.*, 1987). Consequently, the 4-phosphoryl group shows the lowest structural disorder for InsP<sub>3</sub> bound to mPI-PLC (as evident in B-factors). Due to the close and specific interactions of bPI-PLC with the 4- and 5-hydroxyl groups of Ins no space is left to accommodate the bulky phosphate groups of InsP<sub>3</sub>. This explains why bPI-PLC is not able to cleave more highly phosphorylated PIs (Ikezawa, 1991).

No close contacts are found between the 6-hydroxyl of inositol and bPI-PLC or mPI-PLC. Nevertheless, only bPI-PLC can also hydrolyse phosphatidylinositols modified at the 6-hydroxyl such as glycosylphosphatidyl inositols (GPI). In GPIs, the 6-hydroxyl of Ins is modified by a string of four glycan rings. Structural data from the complex of bPI-PLC and glucosaminyl-( $\alpha 1 \rightarrow 6$ )-*myo*-inositol (Heinz *et al.*, 1996) as well as supporting kinetic data (Englund, 1993) indicate that bPI-PLC weakly interacts with the glycan moieties of GPI-anchors, however, not *via* specific contacts. In the structure of bPI-PLC, a wide channel extends from the active site that is formed due to the absence of helices 4 and 5 of the regular TIM-barrel topology. This channel, which is absent in mPI-PLC, could act as a secondary binding site to loosely accommodate some of the glycans present in GPI.

Most of the active site residues do not move upon binding substrate, probably because their side-chains are prestabilized by an intricate network of hydrogen bonding and electrostatic interactions with neighbouring residues. Only the side-chains of Glu341 and Arg549 in mPI-PLC exhibit noticeable conformational change upon complex formation with InsP<sub>3</sub> (Essen *et al.*, 1997). In contrast the conformation and location of amino acids interacting with Ins is essentially unchanged in uncomplexed bPI-PLC (Heinz *et al.*, 1995).

### The catalytic mechanism

From the structures of the complexes, supporting data from enzyme kinetics, and site-directed mutagenesis (Table 4), a sequential catalytic mechanism was proposed for both bPI-PLC (Heinz *et al.*, 1995) and mPI-PLC (Essen *et al.*, 1996, 1997). The reaction proceeds in two steps: a phosphotransfer generates a stable cyclic phosphodiester intermediate and this is followed by a phosphohydrolysis that generates the acyclic inositol phosphate. Apparently, the second step of this two-step mechanism is

sufficiently slow for the bacterial enzyme that the principal product of the reaction is the cyclic intermediate itself. In contrast, the principal product of the eukaryotic PI-PLCs is the acyclic inositol phosphate (Bruzik & Tsai, 1994).

Both enzymes utilize a general base and acid mechanism to catalyse the hydrolysis of phospholipids. However, the structures suggest that the two types of enzymes may use different types of residues to carry out the roles of general acid and base in the catalysis. In the case of bPI-PLC, His32 and His82 were identified as the general base and acid, respectively (Figure 6): His32 is located within hydrogen bonding distance of the 2-OH-group of the inositol and could deprotonate the hydroxyl in a first step. Subsequently, the oxyanion would attack nucleophilically the 1-phosphate group of PI, leading to the formation of a pentacovalent transition state that collapses after protonation by His82 into the products DAG and the stable intermediate Ins(1:2cyc)P. In a second, slower reaction, the roles of both histidine residues are reversed and the nucleophilic attack of an activated hydroxide results in the formation of InsP (Figure 7). The essential role of His32 and His82 for catalysis has been confirmed by site-directed mutagenesis. Replacement of these residues by e.g. leucine leads to a complete inactivation of the enzyme (Table 4).

The mPI-PLC counterparts of the bPI-PLC catalytic histidine residues, His311 and His356, are strictly conserved in all eukaryotic PI-PLCs. Furthermore, their positions and orientations in the active sites of the two enzymes are similar. Nevertheless, the role of His311 as the general base in the first step of the reaction is less clear. Mutation of His311 to leucine leads to a more than 1000-fold reduction in activity (Table 4). This could be attributed to His311 acting as the general base. However in the crystal structures of mPI-PLC in complex with various substrate analogues, His311 does not form the hydrogen bond to the 2-OH-group of InsP<sub>3</sub> as observed between His32 and Ins in bPI-PLC. Instead, His311 interacts with the 1-phosphate group. Therefore it is plausible that His311 is playing a crucial role in the stabilization of the pentacovalent transition state, and that Glu390 or Glu341 might act as the general base (Essen *et al.*, 1997). These residues are not only ligands of the Ca<sup>2+</sup>-cofactor, but also form hydrogen bonds to the 2-OH group of InsP<sub>3</sub>. The corresponding amino acid to Glu390 in mPI-PLC is Lys115 in bPI-PLC, therefore ruling out this as an alternative catalytic base for bPI-PLC. Further biochemical studies are necessary to establish the identity of the general base in mPI-PLC. Along these lines, it was proposed that Asp274 in bPI-PLC enhances the role of His32 as a general base by forming a hydrogen bond with atom ND1 of His32 in a way that resembles the charge relay system found in the catalytic triads of serine proteinases and esterases (Heinz *et al.*, 1995). Mutation of Asp274 to serine leads to an almost complete abolishment of activity (Table 4). In mPI-PLC the residue equivalent to

Asp274 is Asn578. This residue would be much less suitable to stabilize an imidazolium cation of His311 formed during catalysis, although some examples of operating His-Asn pairs are known (Vernet *et al.*, 1995; Hendle *et al.*, 1995). If a mutation of Asn578 to aspartate in mPI-PLC showed enhanced activity, this would suggest that His311 of mPI-PLC is acting as the general base for the first step of the reaction.

A hallmark in the active site of mPI-PLC is the presence of a catalytically essential Ca<sup>2+</sup> that is coordinated to the side-chains of Asn312, Asp343, Glu341 and Glu390, as well as a water molecule and the 2-OH-group of InsP<sub>3</sub>. Besides a possible feedback regulatory role, the Ca<sup>2+</sup> is probably involved in lowering the pK<sub>a</sub> of the 2-OH-group of PIP<sub>2</sub> and stabilizing the pentacovalent transition state during catalysis by both electrostatic interactions and by specific ligation of oxygen atoms of the 1-phosphate (Essen *et al.*, 1997). Direct bidentate ligation of the cyclic intermediate by Ca<sup>2+</sup> may explain why mPI-PLC does not release the cyclic intermediate as readily as bPI-PLC and yields the acyclic inositol phosphate as a major reaction product (Essen *et al.*, 1997).

In contrast, due to very low affinity for the cyclic inositol phosphate ( $K_M = 90$  mM; Zhou *et al.*, 1997) the metal independent bPI-PLC releases most of the cyclic intermediate before completing the second step of the reaction. The electrostatic stabilisation of the transition state in bPI-PLC is accomplished by a basic residue, Arg69. This residue stereospecifically interacts with the phosphate moiety of the substrate (Hondal *et al.*, 1997). In the structure of bPI-PLC, the positively charged guanidinium group of Arg69 fills almost exactly the space that Ca<sup>2+</sup> occupies in the active site of mPI-PLC. Mutation of Arg69 to lysine leads to a complete inactivation of bPI-PLC (Table 4; Hondal *et al.*, 1997). We also constructed the double mutant R69D/K115E in bPI-PLC in order to investigate whether bPI-PLC can be changed to a Ca<sup>2+</sup>-dependent enzyme in analogy to mPI-PLC. Although the mutant could be obtained in a correctly folded form, it showed no detectable catalytic activity in either the absence or presence of Ca<sup>2+</sup>. These data showed that the Ca<sup>2+</sup>-binding site in mPI-PLC probably critically depends on stringent steric and electronic requirements that cannot be achieved in the double mutant.

The GPI-PLC from *T. brucei* is like its bacterial counterpart Ca<sup>2+</sup>-independent (Carrington *et al.*, 1991). Consequently, it lacks the calcium ligands found in other eukaryotic PI-PLCs, but has an arginine residue homologously positioned to Arg69 in bPI-PLC.

### Modelling phospholipid interactions in the active site

Given the exquisite stereospecificity of interaction between the enzyme and *myo*-inositols observed in the crystal structures, it is likely that

PI and PIP<sub>2</sub> bind in a similar fashion to the active sites of bPI-PLC and mPI-PLC. In addition to the stereospecific interactions with the inositol head groups the enzymes probably form a number of van der Waals and hydrophobic interactions between amino acids located in a hydrophobic ridge at the rim of the active site (Figure 8) and the lipophilic tails of the fatty acids. This is supported

by the observed binding of a detergent molecule CHAPSO to this hydrophobic ridge in the crystal structure of mPI-PLC (Essen *et al.*, 1996). The hydrophobic ridge is mainly formed by loops connecting  $\beta$ i and  $\alpha$ 1,  $\beta$ II and  $\alpha$ 2 as well as  $\beta$ VII and  $\alpha$ 7 in both enzymes and contains a number of hydrophobic amino acids exposed to the surface (L320, Y358, F360, W555 and atom C<sup>72</sup> of T557 in

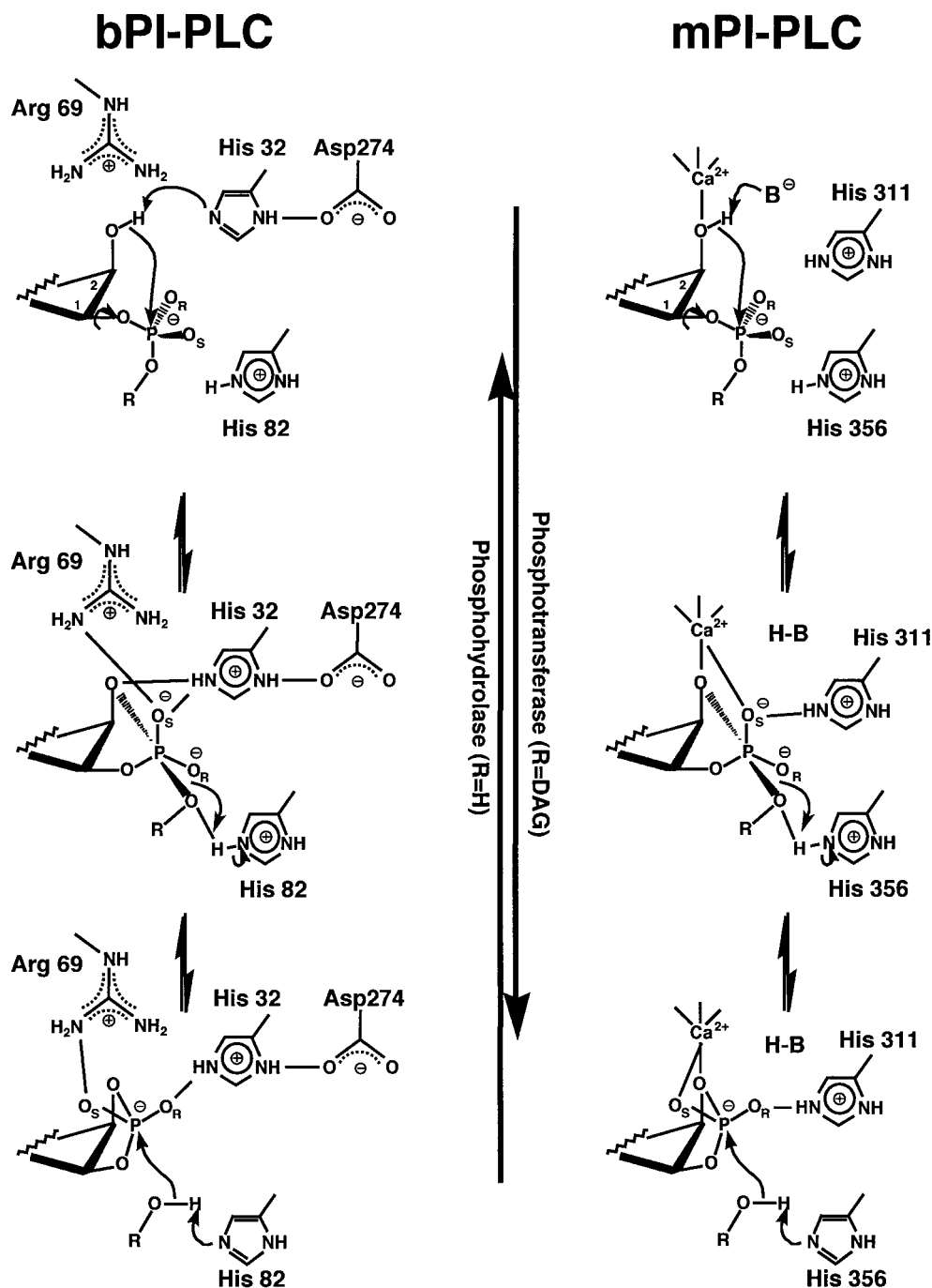


**Figure 7.** Proposed two-step reaction mechanism for the general acid/general base catalysis for bPI-PLC (left) and mPI-PLC (right). For the discussion of the identity of the general base (B<sup>-</sup>) in mPI-PLC see the text. According to structural data of the complexes between bPI-PLC and inositol analogues supported by biochemical data (Hondal *et al.*, 1997), the N<sup>E1</sup>-atom of Arg69 is probably in close proximity to the proximal O<sub>S</sub>-atom of the transition state whereas atom N<sup>E2</sup> is closer to the developing negative charge on the 2-OH-group of the inositol.

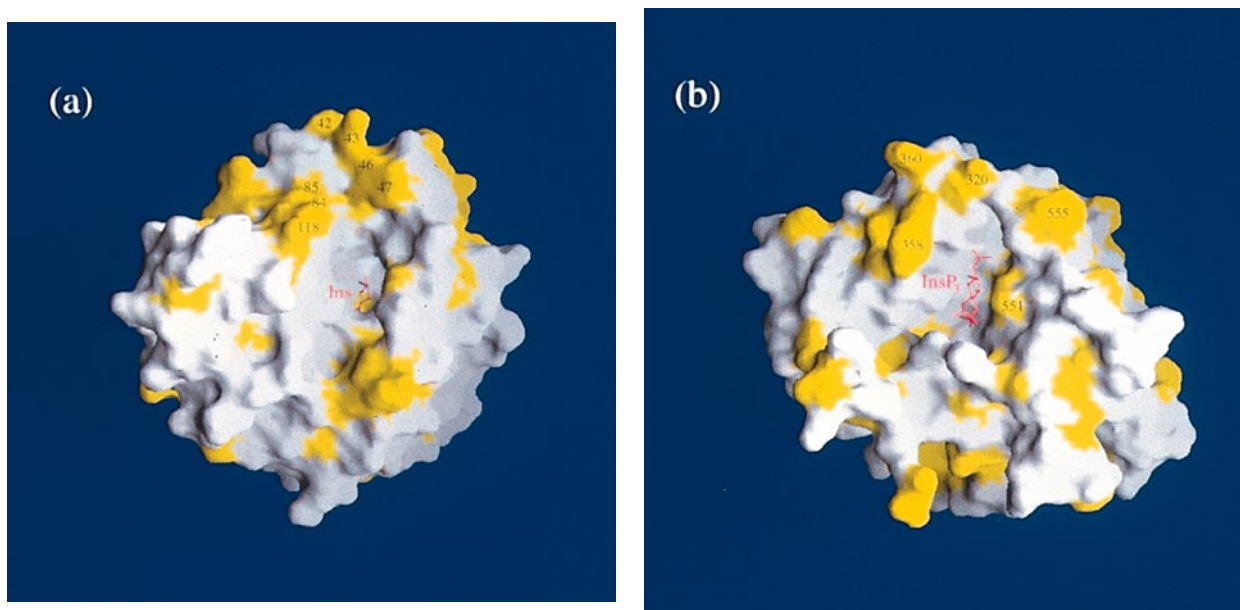


**Figure 8.** Molecular surface representation of PI-PLCs viewing towards the active site (made with GRASP; Nicholls, 1992) with Ins and InsP<sub>3</sub> (coloured in red) bound to the respective active sites. The surfaces corresponding to hydrophobic amino acids are coloured in yellow. Amino acids located in the hydrophobic rim (see the text) are labelled. (a) bPI-PLC with Ins; (b) mPI-PLC with InsP<sub>3</sub>.

mPI-PLC; P42, I43, V46, W47, P84, L85 and Y118 in bPI-PLC; Figure 8). The size of hydrophobic surface (approx. 350 Å<sup>2</sup>) roughly corresponds to an estimate of the membrane penetration area determined by correlating mPI-PLC activity and surface pressure (Boguslavsky *et al.*, 1994). Figure 9 shows a hypothetical model of bPI-PLC and mPI-PLC interacting with a phospholipid membrane. In this

model both enzymes partly penetrate the membrane bilayer to gain access to the substrate. However, the degree of penetration is currently unclear and might be different between the two enzymes. In mPI-PLC, diffusion of head groups into the active site can proceed through a spout-like opening between the membrane and the membrane-docked enzyme (Essen *et al.*, 1997). No such sub-

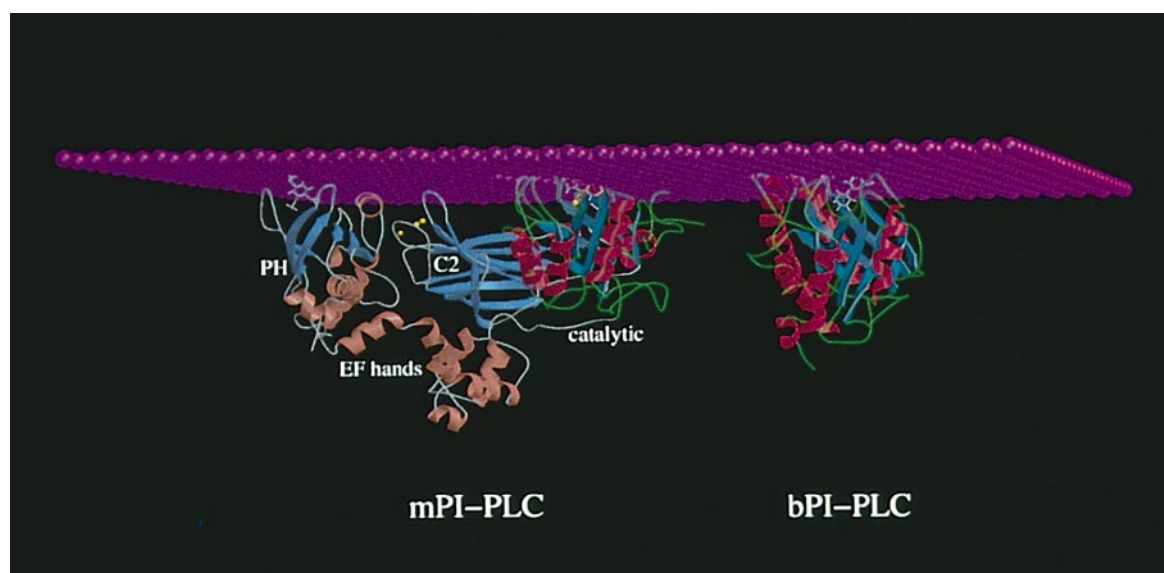


**Figure 9.** Hypothetical model of the interaction of mPI-PLC and bPI-PLC with a phospholipid membrane represented by a layer of spheres. Each sphere corresponds to the head group of a phospholipid molecule that occupies an average area of 0.7 nm<sup>2</sup> on the membrane surface. The catalytic domains of both enzymes have been positioned so that the hydrophobic ridge at the rim of the active site partially penetrates into the membrane. The model of mPI-PLC has been positioned so that the Ca<sup>2+</sup>-binding loops of the C2 domain are also near the membrane. The PH domain of PLC- $\delta$ 1 is shown bound to a PIP<sub>2</sub> headgroup and was positioned so that this headgroup was near the membrane. The placement of the PH domain with respect to the mPI-PLC model was arbitrary with the only constraint that the N terminus of mPI-PLC be near the C terminus of the PH domain.

strate entrance is apparent for bPI-PLC and one might consider a partial pullout mechanism at least for the GPI substrates which carry the bulky glycoprotein modification at the 6-hydroxyl group of the inositol.

Unlike other prokaryotic and eukaryotic PI-PLCs, the *T. brucei* GPI-PLC behaves like a membrane-resident protein that cannot dissociate from lipid membranes in a reversible manner (Bulow *et al.*, 1989). Interestingly, the sequence alignment (Figure 5) shows for the N-terminal half of *T. brucei* GPI-PLC the insertion of a largely hydrophobic segment of 31 amino acids between  $\beta$ -strand  $\beta$ I and  $\alpha$ -helix  $\alpha$ 1 that is predicted to be in an  $\alpha$ -helical conformation. It might be this hydrophobic segment that is responsible for the observed irreversible anchoring of *T. brucei* GPI-PLC to lipid membranes.

## Summary

Despite many structural similarities between bPI-PLC and the catalytic domain of mPI-PLC, the mechanism of both enzymes differs in two respects: the eukaryotic enzymes require a calcium cofactor whereas the bacterial PI-PLCs as well as *T. brucei* GPI-PLC are metal independent; and the principal reaction products of the eukaryotic PI-PLCs are both cyclic and acyclic inositol phosphates while the bacterial enzyme yields mainly the cyclic product. Furthermore, the structures of complexes of these enzymes with substrate analogues have suggested that these enzymes may employ different types of residues to carry out the catalysis.

The comparison of a prokaryotic and eukaryotic PI-PLC structure in combination with multiple sequence alignments suggest a divergent evolution starting from a common ancestor molecule rather than convergent evolution to a stable fold. In the case of bacterial PI-PLCs, the molecule kept its size and single domain structure and probably evolved towards achieving a maximum catalytic efficiency. In eukaryotic PI-PLCs, additional domains and the requirement of a calcium cofactor were incorporated to allow the fine-tuned regulation of PI-PLC *via* specific contacts with receptors, receptor-associated proteins and membranes to establish its role as a central enzyme in most signal transduction pathways.

An alternative evolutionary scenario can be proposed for bacterial PI-PLCs due to the fact that the natural substrate membrane lipid PI is absent in most bacteria (Bishop *et al.*, 1967; Ames, 1968) with the exception of some ice-nucleating bacteria (Kozloff *et al.*, 1984, 1991), suggesting that most bacteria do not require PI-PLC for their own survival (Camilli *et al.*, 1991). In the case of animal and human pathogens, PI-PLC acts as a virulence factor to facilitate infection of their respective hosts. This is corroborated by the fact that no PI-PLC activity is detected in avirulent *Listeria* strains (Notermans *et al.*, 1991). It is plausible that bacterial PI-PLCs might be descendants from eukaryotic PI-PLCs that were incorporated by the bacteria during evol-

ution and later changed by purging additional domains and by optimizing the C-terminal half of the barrel, i.e. the former Y region. In contrast, the N-terminal half of the barrel that contributes most of the active site residues would have been more constrained in its evolution. In this scenario, the loss of a requirement for a  $\text{Ca}^{2+}$ -cofactor would have been selected for in bacteria living as intracellular parasites because the resting  $\text{Ca}^{2+}$  concentration in the host eukaryotic cells would likely be limiting for efficient catalysis.

## Materials and Methods

### Structural alignment and multiple sequence alignment

The structures were superimposed using either the routines *lsq\_explicit* and *lsq\_improve* in program O (Jones *et al.*, 1991), the program GA\_FIT (May & Johnson, 1994) or the program SUPERIMPOSE (Diederichs, 1995).

The program PILEUP in the GCG package (Devereux *et al.*, 1984) was used to perform multiple sequence alignments separately for both eukaryotic and prokaryotic PI-PLCs. The alignment between the bPI-PLC (residues 1 to 298) and the catalytic domain of mPI-PLC (residues 290 to 606) was adjusted manually based on the crystal structures. All sequences were obtained from the SWISS-PROT Data Base *via* the GCG package. For the alignment of the catalytic domains, the following sequences were used: PI-PLC from *Drosophila* (*pipa\_drome*, residues 323 to 663), PI-PLC from yeast (*pip1\_yeast*, residues 384 to 707), PI-PLC- $\delta$ 1 from rat (*pip6\_rat*, residues 300 to 606), PI-PLC- $\beta$ 1 from rat (*pip1\_rat*, residues 320 to 653), human PI-PLC- $\gamma$ 1 (*pip4\_human*, residues 324 to 1067), PI-PLC from *T. brucei* (*phlc\_trybb*, residues 6 to 336), PI-PLC from *B. cereus* (*plc\_bacce*, residues 1 to 298) and PI-PLC from *L. monocytogenes* (*plc\_lismo*, residues 1 to 286).

### Surface areas

Accessible surface areas of inositols in free form and bound to the enzymes were calculated using the program of Connolly (1983) using a radius for the probing sphere of 1.4 Å and the default radii of GRASP (Nicholls, 1992).

## Acknowledgements

We thank Dr Olga Perisic for valuable discussion and comments on the manuscript. The support of the Deutsche Forschungsgemeinschaft, Bonn, Germany (to D.W.H.), the British Heart Foundation (to R.L.W.) and the MRC/DTI/ZENECA LINK Programme (to R.L.W.) are gratefully acknowledged.

## References

- Ames, G. F. (1968). Lipids of *Salmonella typhimurium* and *Escherichia coli*: structure and metabolism. *J. Bacteriol.* **95**, 833–843.
- Berridge, M. J. (1993). Inositol trisphosphate and calcium signalling. *Nature*, **361**, 315–325.

- Bishop, D. G., Rutberg, L. & Samuelsson, B. (1967). The chemical composition of the cytoplasmic membrane of *Bacillus subtilis*. *Eur. J. Biochem.* **2**, 448–453.
- Boguslavsky, V., Rebecchi, M., Morris, A. J., Jhon, D.-Y., Rhee, S. G. & McLaughlin, S. (1994). Effect of monolayer surface pressure on the activities of phosphoinositide-specific phospholipase C- $\beta$ 1, - $\gamma$ 1, and - $\delta$ 1. *Biochemistry*, **33**, 3032–3037.
- Bruzik, K. S. & Tsai, M.-D. (1994). Toward the mechanism of phosphoinositide-specific phospholipases C. *Bioorg. Med. Chem.* **2**, 49–72.
- Bruzik, K. S., Morocho, A. M., Jhon, D.-Y., Rhee, S. G. & Tsai, M.-D. (1992). Phospholipids chiral at phosphorus. Stereochemical mechanism for the formation of inositol 1-phosphate catalysed by phosphatidylinositol-specific phospholipase C. *Biochemistry*, **31**, 5183–5193.
- Bruzik, K. S., Hakeem, A. A. & Tsai, M.-D. (1994). Are D- and L-chiro-phosphoinositides substrates of phosphatidylinositol-specific phospholipase C? *Biochemistry*, **33**, 8367–8374.
- Bulow, R., Griffiths, G., Webster, P., Stierhof, Y.-D., Opperdoes, F. R. & Overath, P. (1989). Intracellular localization of the glycosyl-phosphatidylinositol-specific phospholipase C from *Trypanosoma brucei*. *J. Cell. Sci.* **93**, 233–240.
- Bütikofer, P., Boschung, M., Brodbeck, U. & Menon, A. K. (1996). Phosphatidylinositol hydrolysis by *Trypanosoma brucei* GPI phospholipase C. *J. Biol. Chem.* **271**, 15533–15541.
- Cambillau, C. & van Tilbeurgh, H. (1993). Structure of hydrolases: lipases and cellulases. *Curr. Opin. Struct. Biol.* **3**, 885–895.
- Camilli, A., Goldfine, H. & Portnoy, D. A. (1991). *Listeria monocytogenes* mutants lacking phosphatidylinositol-specific phospholipase C are avirulent. *J. Exp. Med.* **173**, 751–754.
- Carrington, M., Walters, D. & Webb, H. (1991). The biology of the glycosyl-phosphatidylinositol-specific phospholipase C of *Trypanosoma brucei*. *Cell Biol. Int. Rep.* **15**, 1101–1114.
- Cheng, H.-F., Jiang, M.-J., Chen, C.-L., Liu, S.-M., Wong, L.-P., Lomasney, J. W. & King, K. (1995). Cloning and identification of amino acid residues of human phospholipase C $\delta$ 1 essential for catalysis. *J. Biol. Chem.* **270**, 5495–5505.
- Connolly, M. L. (1983). Analytical molecular surface calculation. *J. Appl. Crystallog.* **16**, 548–558.
- Daugherty, S. & Low, M. G. (1993). Cloning, expression, and mutagenesis of phosphatidylinositol-specific phospholipase C from *Staphylococcus aureus*: a potential staphylococcal virulence factor. *Infect. Immun.* **61**, 5078–5089.
- Devereux, J., Haerberli, P. & Smithies, O. (1984). A comprehensive set of sequence analysis programs for the VAX. *Nucl. Acids Res.* **12**, 387–395.
- Diederichs, K. (1995). Structural superposition of proteins with unknown alignment and detection of topological similarity using a six-dimensional search algorithm. *Proteins: Struct. Funct. Genet.* **23**, 187–195.
- Ellis, M. V. U. S. & Katan, M. (1995). Mutations within a highly conserved sequence present in the X region of phosphoinositide-specific phospholipase C- $\delta$ 1. *Biochem. J.* **307**, 69–75.
- Englund, P. T. (1993). The structure and biosynthesis of glycosyl phosphatidylinositol protein anchors. *Annu. Rev. Biochem.* **62**, 121–138.
- Essen, L.-O., Perisic, O., Cheung, R., Katan, M. & Williams, R. L. (1996). Crystal structure of a mammalian phosphoinositide-specific phospholipase C $\delta$ . *Nature*, **380**, 595–602.
- Essen, L.-O., Perisic, O., Katan, M., Wu, Y., Roberts, M. F. & Williams, R. L. (1997). Structural mapping of the catalytic mechanism for a mammalian phosphoinositide-specific phospholipase C. *Biochemistry*, **36**, 1704–1718.
- Ferguson, K. M., Lemmon, M. A., Schlessinger, J. & Sigler, P. B. (1995). Structure of the high affinity complex of inositol trisphosphate with a phospholipase C pleckstrin homology domain. *Cell*, **83**, 1037–1046.
- Gässler, C. S., Ryan, M., Liu, T., Griffith, O. H. & Heinz, D. W. (1997). Probing the roles of active site residues in phosphatidylinositol-specific phospholipase C from *Bacillus cereus* by site-directed mutagenesis. *Biochemistry*, **36**, 12,802–12,813.
- Grobler, J. A., Essen, L.-O., Williams, R. L. & Hurley, J. H. (1996). C2 domain conformational changes in phospholipase C- $\delta$ 1. *Nature Struct. Biol.* **3**, 788–795.
- Heinz, D. W., Ryan, M., Bullock, T. L. & Griffith, O. H. (1995). Crystal structure of the phosphatidylinositol-specific phospholipase C from *Bacillus cereus* in complex with myo-inositol. *EMBO J.* **14**, 3855–3863.
- Heinz, D. W., Ryan, M., Smith, M., Weaver, L., Keana, J. & Griffith, O. H. (1996). Crystal structure of phosphatidylinositol-specific phospholipase C from *Bacillus cereus* in complex with glucosamine ( $\alpha$ 1  $\rightarrow$  6) myo-inositol, an essential fragment of GPI-anchors. *Biochemistry*, **35**, 9496–9504.
- Hendle, J., Mattevi, A., Westphal, A. H., Spee, J., de Kok, A., Teplyakov, A. & Hol, W. G. J. (1995). Crystallographic and enzymatic investigations of the role of Ser 558, His 610, and Asn 614 in the catalytic mechanism of *Azotobacter vinelandii* dihydrolipamide acetyltransferase (E2p). *Biochemistry*, **34**, 4287–4298.
- Hereld, D., Hart, G. W. & Englund, P. T. (1988). cDNA encoding the glycosyl-phosphatidylinositol-specific phospholipase C of *Trypanosoma brucei*. *Proc. Natl Acad. Sci. USA*, **85**, 8914–8918.
- Holm, L. & Sander, C. (1993). Protein structure comparison by alignment of distance matrices. *J. Mol. Biol.* **233**, 123–138.
- Hondal, R. J., Riddle, S. R., Kravchuk, A. V., Zhao, Z., Liao, H., Bruzik, K. S. & Tsai, M.-D. (1997). Phosphatidylinositol-specific phospholipase C: Kinetic and stereochemical evidence for an interaction between arginine-69 and the phosphate group of phosphatidylinositol. *Biochemistry*, **36**, 6633–6642.
- Hough, E., Hansen, L. K., Birknes, B., Jynge, K., Hansen, S., Hordvik, A., Little, C., Dodson, E. & Derewenda, Z. (1989). High-resolution (1.5 Å) crystal structure of phospholipase C from *Bacillus cereus*. *Nature*, **338**, 357–360.
- Ikezawa, H. (1991). Bacterial PIPLCs - unique properties and usefulness in studies on GPI anchors. *Cell. Biol. Intl. Rep.* **15**, 1115–1131.
- Jones, T. A., Zou, J.-Y., Cowan, S. W. & Kjeldgaard, M. (1991). Improved methods for building protein models in electron density maps and the location of errors in these models. *Acta Crystallog. sect. A*, **47**, 110–119.
- Kozloff, L. M., Lute, M. & Westaway, D. (1984). Phosphatidylinositol as a component of the ice nucleating site of *Pseudomonas syringae* and *Erwinia herbicola*. *Science*, **226**, 845–846.

- Kozloff, L. M., Turner, M. A., Arellano, F. & Lute, M. (1991). Phosphatidylinositol, a phospholipid of ice-nucleating bacteria. *J. Bacteriol.* **173**, 2053–2060.
- Kraulis, P. J. (1991). MOLSCRIPT: A program to produce both detailed and schematic plots of protein structures. *J. Appl. Crystallog.* **24**, 946–950.
- Kuppe, A., Evans, L. M., McMillen, D. A. & Griffith, O. H. (1989). Phosphatidylinositol-specific phospholipase C of *Bacillus cereus*: cloning, sequencing, and relationship to other phospholipases. *J. Bacteriol.* **171**, 6077–6083.
- Leimeister-Wächter, M., Domann, E. & Chakraborty, T. (1991). Detection of a gene encoding phosphatidylinositol-specific phospholipase C that is co-ordinately expressed with listeriolysin in *Listeria monocytogenes*. *Mol. Microbiol.* **5**, 361–366.
- Lewis, K. A., Garigapati, V. R., Zhou, C. & Roberts, M. F. (1993). Substrate requirements of bacterial phosphatidylinositol-specific phospholipase C. *Biochemistry*, **32**, 8836–8841.
- Martin, S. F. & Wagman, A. S. (1996). Synthesis and kinetic evaluation of inhibitors of the phosphatidylinositol-specific phospholipase C from *Bacillus cereus*. *J. Org. Chem.* **61**, 8016–8023.
- May, A. C. W. & Johnson, M. S. (1994). Protein structure comparisons using a combination of a genetic algorithm, dynamic processing and least-squares minimization. *Protein Eng.* **7**, 475–485.
- McLachlan, A. D. (1979). Gene duplications in the structural evolution of chymotrypsin. *J. Mol. Biol.* **128**, 49–79.
- Mengaud, J., Braun-Breton, C. & Cossart, P. (1991). Identification of phosphatidylinositol-specific phospholipase C activity in *Listeria monocytogenes*: a novel type of virulence factor? *Mol. Microbiol.* **5**, 367–372.
- Merrit, E. A. & Murphy, M. E. P. (1994). Raster3D Version 2.0: a program for photorealistic molecular graphics. *Acta Crystallog. sect. D*, **50**, 869–873.
- Morris, J. C., Ping-Sheng, L., Shen, T.-Y. & Mensa-Wilmot, K. (1995). Glycan requirements of glycosyl phosphatidylinositol phospholipase C from *Trypanosoma brucei*. *J. Biol. Chem.* **270**, 2517–2524.
- Moser, J., Gerstel, B., Meyer, J. E. W., Chakraborty, T., Wehland, J. & Heinz, D. W. (1997). Crystal structure of the phosphatidylinositol-specific phospholipase C from the human pathogen *Listeria monocytogenes*. *J. Mol. Biol.* **273**, 269–282.
- Nicholls, A. (1992). *GRASP: Graphical representation and analysis of surface properties*, Columbia University, USA, NY.
- Nishizuka, Y. (1992). Intracellular signaling by hydrolysis of phospholipids and activation of protein kinase C. *Science*, **258**, 607–614.
- Notermans, S. H. W., Dufrenne, J., Leimeister-Wächter, M., Domann, E. & Chakraborty, T. (1991). Phosphatidylinositol phospholipase C activity as a marker to distinguish between pathogen and non-pathogenic *Listeria* species. *Appl. Environ. Microbiol.* **57**, 2666–2670.
- Potter, B. V. L. & Lampe, D. (1995). Chemistry of inositol lipid mediated cellular signaling. *Angew. Chem. Int. Ed. Engl.* **34**, 1933–1972.
- Quiucho, F. A. (1989). Protein-carbohydrate interactions: basic molecular features. *Pure Appl. Chem.* **61**, 1293–1306.
- Reardon, D. & Farber, G. K. (1995). The structure and evolution of  $\alpha/\beta$  barrel proteins. *FASEB J.* **9**, 497–503.
- Rhee, S. G., Suh, P.-G., Ryu, S.-H. & Lee, S. Y. (1989). Studies of inositol phospholipid-specific phospholipase C. *Science*, **244**, 546–550.
- Rouvinen, J., Bergfors, T., Knowles, J. K. C. & Jones, T. A. (1990). Three-dimensional structure of cellobiohydrolase II from *Trichoderma reesei*. *Science*, **249**, 380–386.
- Ryu, S. H., Suh, P.-G., Cho, K. S., Lee, K.-Y. & Rhee, S. G. (1987). Bovine brain cytosol contains three immunologically distinct forms of inositol phospholipid-specific phospholipase C. *Proc. Natl Acad. Sci. USA*, **84**, 6649–6653.
- Scott, D. L., White, S. P., Otwinowski, Z., Yuan, W., Gelb, M. H. & Sigler, P. B. (1990). Interfacial catalysis: the mechanism of phospholipase A<sub>2</sub>. *Science*, **250**, 1541–1546.
- Serunian, L. A., Haber, M. T., Fukui, T., Kim, J. W., Rhee, S. G., Lowenstein, J. M. & Cantley, L. C. (1989). Polyphosphoinositides produced by phosphatidylinositol 3-kinase are poor substrates for phospholipases C from rat liver and bovine brain. *J. Biol. Chem.* **264**, 17809–17815.
- Simões, A. P., Camps, M., Schnabel, P. & Gierschik, P. (1995). Mutational analysis of a putative polyphosphoinositide binding site in phospholipase C- $\beta$ 2. *FEBS Letters*, **365**, 155–158.
- Smith, M. R., Liu, Y.-L., Matthews, N. T., Rhee, S. G., Sung, W. K. & Kung, H.-F. (1994). Phospholipase C- $\gamma$ 1 can induce DNA synthesis by a mechanism independent of its lipase activity. *Proc. Natl Acad. Sci. USA*, **91**, 6554–6558.
- Spezio, M., Wilson, D. B. & Karplus, P. A. (1993). Crystal structure of the catalytic domain of a thermophilic endocellulase. *Biochemistry*, **32**, 9906–9916.
- Vernet, T., Tessier, D. C., Chatellier, J., Plouffe, C., Lee, T. S., Thomas, D. Y., Storer, A. C. & Ménard, R. (1995). Structural and functional roles of asparagine 175 in the cysteine proteinase papain. *J. Biol. Chem.* **270**, 16645–16652.
- Wang, L.-P., Lim, C., Kuan, Y.-S., Chen, C.-L., Chen, H.-F. & King, K. (1996). Positive charge at position 549 is essential for phosphatidylinositol 4,5-bisphosphate-hydrolyzing but not phosphatidylinositol-hydrolyzing activities of human phospholipase C $\delta$ 1. *J. Biol. Chem.* **271**, 24505–24516.
- White, S. P., Scott, D. L., Otwinowski, Z., Gelb, M. H. & Sigler, P. B. (1990). Crystal structure of cobra venom phospholipase A<sub>2</sub> in a complex with a transition-state analogue. *Science*, **250**, 1560–1563.
- Williams, R. L. & Katan, M. (1996). Structural views of phosphoinositide-specific phospholipase C: signaling the way ahead. *Structure*, **4**, 1387–1394.
- Zhou, C., Wu, Y. & Roberts, M. F. (1997). Activation of phosphatidylinositol-specific phospholipase C toward inositol 1,2-(cyclic)-phosphate. *Biochemistry*, **36**, 347–355.

Edited by K. Nagai

(Received 11 June 1997; received in revised form 1 October 1997; accepted 27 October 1997)